

Green Synthesis, Characterization and Antibacterial and Leishmanicidal Activities of Silver Nanoparticles Obtained from Aqueous Extract of *Eucalyptus grandis*

Lucas M. F. Oliveira,^a Ueveton P. da Silva,^a João Pedro V. Braga,^b Álvaro V. N. C. Teixeira,^c Andréa O. B. Ribon,^b Eduardo V. V. Varejão,^a Eduardo A. F. Coelho,^d Camila S. de Freitas,^d Róbson R. Teixeira^a and Renata P. L. Moreira^{✉*}

^aDepartamento de Química, Universidade Federal de Viçosa, 36570-000 Viçosa-MG, Brazil

^bDepartamento de Bioquímica e Biologia Molecular, Universidade Federal de Viçosa, 36570-000 Viçosa-MG, Brazil

^cDepartamento de Física, Universidade Federal de Viçosa, 36570-000 Viçosa-MG, Brazil

^dFaculdade de Medicina, Universidade Federal de Minas Gerais, 30130-100 Belo Horizonte-MG, Brazil

This work describes a green synthesis, the characterization, and biological evaluation of silver nanoparticles (AgNPs). The AgNPs suspension was synthesized using aqueous leaf extract of *Eucalyptus grandis*, which presented a characteristic band at 407 nm in the UV-Vis spectrum. The AgNPs presented a spherical shape and size of 9.7 ± 0.3 nm. The nanoparticles were stable over a month, indicating that *E. grandis*' extract is suitable for their preparation and stabilization. The X-ray analysis showed that the crystallinity of AgNPs corresponded to the centered face phase of silver. The antibacterial and leishmanicidal activities of AgNPs were evaluated. The AgNPs presented antibacterial activity on the Gram-negative bacteria *Escherichia coli* at $53.9 \mu\text{g mL}^{-1}$. The leishmanicidal activity evaluation against promastigote forms of *Leishmania infantum*, *Leishmania amazonensis*, and *Leishmania braziliensis* showed that the biological response is dependent on the volume of AgNP suspension. It was demonstrated that *L. infantum* was more sensitive to the nanoparticle's treatment than *L. amazonensis* and *L. braziliensis*. The treatment of *L. infantum* promastigotes with 150 μL of AgNP suspension reduced parasite growth by 67.9%, a result which was similar to the treatment with 1 (66.7%) or 2 μL (70.6%) of amphotericin B used as a positive control.

Keywords: silver nanoparticles, green synthesis, antibacterial, leishmanicidal, *Eucalyptus grandis*

Introduction

Nanoparticles (NPs) are materials that have at least one dimension between 1 and 100 nm presenting different properties compared to those with the same composition, but having a particle size in a micrometric scale or larger.¹ The applications of NPs are related to their high surface area/volume ratio which confers to them diverse and desirable physical and chemical properties including an increase in reactivity and catalytic efficiency, optical absorption, electrical conductivity, mechanical strength, and magnetic properties.² Thus, NPs can be applied as catalysts,³ biochemical sensors,⁴ in electronic equipment,⁵

data storage devices,⁶ as drug carriers, in tumor imaging systems,⁷ and medical treatments.⁸

Metals such as gold, silver, and copper are noteworthy among the constituents of NPs due to their intrinsic characteristics that enhance applications in electro-electronics and the phenomenon of localized surface plasmon resonance (LSPR). The LSPR phenomenon is the collective oscillation of conducting electrons confined to the surface of a metallic particle in resonance with an incident electromagnetic wave. It results in intense scattering and/or absorption of this radiation. LSPR is a relevant phenomenon because it allows the use of metallic nanoparticles as optical sensors.⁹

Silver stands out among metals because it has a more intense LSPR over a wider range of the electromagnetic spectrum.¹⁰ In addition, silver nanoparticles (AgNPs)

*e-mail: renata.plopes@ufv.br

Editor handled this article: Izaura Cirino Nogueira Diógenes (Associate)

have antimicrobial properties, which make them a therapeutic alternative to face antimicrobial resistance.¹¹ Besides, leishmanicidal activity has also been reported for AgNPs.^{12,13}

AgNPs can be produced and stabilized, generally, by two approaches: top-down or bottom-up. The top-down strategy consists of synthesizing the nanostructure by physical wear of macroscopic materials, whether by grinding, spraying, laser ablation, or lithography, among others. However, it is an energy-expensive and low-yield approach for producing nanoparticles. In the bottom-up strategy, the nanostructure is synthesized by chemical or biological processes so that atoms are organized to form the particle, for example, by chemical or photochemical reduction.¹⁴

The bottom-up processes to produce AgNPs are preferred because they are more energy efficient, allow for better control over the product's characteristics by modulating the synthesis conditions, and present high yields. However, it is common in the bottom-up processes the use of reagents that pose risks to the environment and human health, such as hydrazine and potassium bitartrate, which reduces the biocompatibility of the produced nanoparticles and restricts possible biomedical applications. Therefore, the development of environmentally friendly methods, which allows the control of morphology and stability, has been the focus of recent research.¹

Processes that use reducing agents of biological origin (vegetable or microbial) or that take advantage of the metabolism of microorganisms such as bacteria, fungi, and algae to produce AgNPs, have emerged as an alternative to conventional synthetic processes since they agree with the principles of green chemistry.¹⁵ Compared to methods that utilize microorganisms, methodologies that use plant extracts do not require the steps of isolation, cultivation, and maintenance of the microbial culture as well as do not require aseptic conditions. Furthermore, the reactions are usually faster, more cost-effective, and more easily scalable for industrial purposes.^{14,16}

Eucalyptus (family Myrtaceae) is a genus of perennial fast-growing plants, consisting of shrubs and trees. Around the world, more than 800 species have been identified, the majority being endemic to Australia, but it is currently cultivated in almost all tropical and subtropical regions. In Brazil, *Eucalyptus grandis* is widely cultivated and used for the production of cellulose and paper and, generally, its leaves constitute an industrial waste.^{17,18}

Considering the premises, the purpose of this work was to develop a green synthesis procedure for the preparation of AgNPs by using the leaf aqueous extract of *E. grandis*. Since this vegetable species is widely cultivated in

Brazil, we envisioned that the extract would be a good and readily available reducing agent to synthesize the AgNPs. It is possible to find in the literature reports¹⁹⁻²⁵ of AgNPs being synthesized by extracts from other species of *Eucalyptus*. However, to the best of our knowledge, this is the first report using *E. grandis*. Considering the interest of our research group in finding new antibacterial and leishmanicidal therapeutic alternatives, we also evaluated the activity of the AgNPs against two bacterial and three leishmania species. Although there are reports in the literature concerning the evaluation of these activities for AgNPs, we hypothesized that the properties of AgNPs synthesized from *E. grandis* may differ from those previously described, and, therefore, they would present different antibacterial and leishmanicidal profiles. The results of the biological evaluation of AgNPs herein synthesized are also described.

Experimental

Reagents and chemicals

Ethyl acetate (99.5%), methanol (99.8%), sulfuric acid (95%), and glycerin (99.5%) were purchased from Alphatec (São Bernardo do Campo, São Paulo, Brazil). Silver nitrate (99.9%) and sodium hydroxide (99.6%) were procured from Neon (Suzano, São Paulo, Brazil). Anhydrous magnesium sulfate (98%) and potassium hydroxide (85%) from Vetec (Rio de Janeiro City, Rio de Janeiro State, Brazil). Potassium chromate (99.5%) and sodium chloride (99%) from Merck (São Paulo City, São Paulo State, Brazil). All aqueous solutions were prepared with type 1 water obtained by the Milli-Q system (Bedford, USA), unless otherwise stated.

Plant material

Leaves of *E. grandis* were collected at the campus of the Federal University of Viçosa (UFV) in February 2020, properly washed with distilled water, and oven-dried at 60 °C for 48 h. This long period of time was used to ensure the drying of the sample. The dried plant material was ground in a blade mill and stored at 4 °C until used.

Preparation of plant extract

The aqueous extract from the plant material was prepared based on the procedure reported by Sila *et al.*²⁵ A flask was charged with 10.00 mL of deionized water at 90 °C and 0.100 g of plant material. The resulting mixture was stirred for 5 min. After that, the system was filtered

using qualitative filter paper and the obtained filtrate was centrifuged at 2500 rpm for 10 min. The supernatant was collected and used for the production of nanoparticles (*vide infra*).

Identification of chemical constituents from leaves of *E. grandis*

The chemical composition of the plant material was investigated by infrared spectroscopy (IR) and gas chromatography coupled with mass spectrometry (GC-MS) analyses. Attenuated total reflectance-Fourier transform infrared (ATR-FTIR) spectra were obtained using a Varian 660-IR spectrometer (Palo Alto, USA). Plant material (0.500 g) was subjected to maceration using methanol (10.00 mL) for 30 min. The extract was filtered, dried over anhydrous Na₂SO₄, and concentrated under reduced pressure at 40 °C. Before GC-MS analysis, the extract was subjected to silylation using *N,O*-bis(trimethylsilyl) trifluoroacetamide (BSTFA) (Sigma-Aldrich, St. Louis, MI, USA), according to the methodology reported by da Silva *et al.*²⁶ The derivatized extract was then subjected to GC-MS analysis using a Shimadzu GCMS-QP5050A equipment (Shimadzu, Kyoto, Japan) under the following operating conditions: electron impact method (70 eV); scan mode, *m/z* 30.00 to 700.00; RTx5 capillary column (30 m × 0.25 mm, 0.25 μm); carrier gas flow (He), 1 mL min⁻¹; 1:5 split ratio; injector temperature, 290 °C; detector temperature, 290 °C; sample injection volume was 1.0 μL with a 1:3 split ratio; initial temperature of 80 °C for 5 min and gradient at 4 °C min⁻¹ to 300 °C. Compounds were identified by comparing their mass spectra with data from the equipment (Nist-11 and Wiley-7 libraries) and their calculated retention indexes with those reported in the literature.^{27,28} Only compounds with mass spectra presenting a similarity index of at least 90% similarity with those from the library of the equipment are reported as identified.

Synthesis and characterization of AgNPs

An aqueous solution of silver nitrate (10 mmol L⁻¹) was prepared, previously standardized by the Mohr method, and stored under refrigeration (4 °C) until use. The synthesis of silver nanoparticles was performed as follows: 20 mL of the aqueous extract from the leaves of *E. grandis* was diluted to 47.5 mL and the pH was adjusted to 9.0 with H₂SO₄ or NaOH solutions, both at 0.1 mol L⁻¹. The system was left at room temperature (ca. 25 °C) in the dark for 48 h before being used. Subsequently, the system was heated to 45 °C and an aqueous solution of silver nitrate was added so that the final concentration of Ag was equal to 0.5 mmol L⁻¹ (or

26.9 μg mL⁻¹) remaining at this temperature for 1 h. The AgNPs suspension obtained was stored at room temperature (ca. 25 °C) protected from light. Assuming the reduction of all silver ions, the mass concentration of nanoparticles obtained was equal to 26.9 μg mL⁻¹.

The absorption spectrum of the AgNPs suspension was obtained using a Thermo Scientific model Evolution Array molecular absorption spectrophotometer (Waltham, Massachusetts, USA). A 10 mm optical path quartz cuvette was used. Previously the analysis, the AgNP suspension was diluted 10 times.

Dynamic light scattering (DLS) measurements were performed on the Brookhaven Co. instrument (Holtsville, New York, USA) equipped with the BI-200SM system, 522-channel TurboCorr correlator, and using correlation times up to 100 ns. The light source was a HeNe laser, with a wavelength of 632.8 nm and a power of 75 mW. The monitoring and treatment of data were carried out by the BIC Dynamic Light Scattering Software,²⁹ and the NNLS (non-negative least-squares) model was used to adjust the correlation function.

The X-ray diffractogram was obtained using a Bruker instrument (Billerica, Massachusetts, USA), model D8-Discover. The sample was dropped onto a microscope slide and allowed to dry at room temperature in the dark. The peaks were analyzed with the help of the Search-Match software.³⁰ The measurements were performed using a copper tube (1.5406 Å) and a speed of 1° min⁻¹, in the angular range of 2θ = 25 to 75°.

Transmission electron microscopy (TEM)/energy dispersion spectroscopy (EDS) analyses were performed using a JEM-2100, JEOL (Akishima, Tokyo, Japan) equipment presenting a LaB6 electron emission source and operated with an electron acceleration voltage of 200 kV. For the analysis, the sample was dropped onto a copper grid covered with a Formvar film and carbon deposit.

Antimicrobial activity assay

Biological assays were performed with the following bacterial strains: Gram-positive *Staphylococcus aureus* NRS 155 and Gram-negative *Escherichia coli* ATCC 29214. These species are commonly used in antibacterial activity tests due to morphological differences between these two groups that can affect the antibacterial activity of a tested compound. Bacteria was streaked on brain-heart agar (BHA; Merck, Germany) plates and kept for 24 h at 37 °C. Bacterial suspensions of 0.5 McFarland standard turbidity were prepared and added to sterile tubes containing Mueller Hinton (Kasvi, Brazil) broth to yield an inoculum containing 10⁶ colony forming unit (CFU) mL⁻¹.

Then, the aqueous extract from leaves of *E. grandis*, the suspension of AgNPs ($26.9 \mu\text{g mL}^{-1}$), AgNP suspension with twice the Ag mass concentration of the original ($53.9 \mu\text{g mL}^{-1}$) (AgNPs-2), an aqueous solution of silver nitrate ($26.9 \mu\text{g mL}^{-1}$) or, as a positive control, distilled water was added. Tubes containing an aqueous solution of silver nitrate were also prepared. The tubes were kept at 37°C for 16 h and then the cultures were serially diluted, and a micro drop ($10 \mu\text{L}$) was plated onto BHA for bacterial cell count. Assays were performed in triplicates.

Analysis of variance (ANOVA) was used to statistically analyze the treated groups and Duncan's test was applied to identify the differences between treated groups and the respective control. The data were considered significant at $p \leq 0.05$ level.

Leishmanicidal activity assay

Leishmania infantum (MHOM/BR/1970/BH46), *Leishmania braziliensis* (MHOM/BR/75/M2904), and *Leishmania amazonensis* (IFLA/BR/1967/PH-8) promastigotes were grown in complete Schneider's medium (Sigma-Aldrich, Saint Louis, USA), which was composed by medium plus 20% heat-inactivated fetal bovine serum (FBS; Sigma-Aldrich, Saint Louis, USA), 20 mmol L^{-1} of L-glutamine, 200 U mL^{-1} of penicillin, 100 $\mu\text{g mL}^{-1}$ of streptomycin, and 50 $\mu\text{g mL}^{-1}$ of gentamicin pH 7.4, at 24°C .³¹ The protocol to evaluate the antileishmanial activity was adapted from Awad *et al.*¹² Briefly, *L. infantum*, *L. braziliensis*, and *L. amazonensis* stationary promastigotes (2×10^5 parasites *per well*) were kept in 100 μL of Roswell Park Memorial Institute (RPMI) medium in 96-well plates for 24 h at 24°C . Then, AgNPs (10, 50, 80, 100 and 150 μL) or amphotericin B (1, 2 and 4 μL ; 10 mg mL^{-1}) were added to wells and the final volume was adjusted for 250 μL in each well by using RPMI medium. Treated parasites were kept in incubation for 48 h at 24°C . Next, 3-(4,5-dimethylthiazol-2-yl)-2,5-diphenyl-tetrazolium bromide (MTT; Sigma-Aldrich, Saint Louis, USA), which was previously sterilized through a 0.22 μm filter, was added to a final concentration of 5 mg mL^{-1} (10 μL in each well) and cultures were kept in the dark for 3 h at 26°C . Then, plates were centrifuged using 3500 \times rpm for 20 min at 24°C , in order to remove the medium plus MTT. Afterwards, 100 μL dimethyl sulfoxide (DMSO) were added to each well, and the plates were kept in the dark for 15 min at 24°C , to dissolve the formazan crystals. The optical density (OD) values were read in a microplate spectrophotometer (Molecular Devices, Spectra Max Plus, San Jose, CA, USA), at 570 nm. Experiments were repeated twice and presented similar results.

Results and Discussion

Plant extract characterization

Plant extracts are a complex mixture of substances that originate from plant metabolism and are transferred to a solvent during the extraction process.³² They are used in the synthesis of NPs due to the presence of compounds that act as reducing and stabilizing agents which prevent aggregation.¹⁵ In the present investigation, we utilized the aqueous extract from leaves of *E. grandis* as a reducing agent to prepare AgNPs. The chemical composition of the extract from the aforementioned plant species was investigated via IR and GC-MS techniques. For these purposes, methanolic extracts were prepared. The infrared spectrum of leaf of *E. grandis* (Figure 1) shows a band at 3363 cm^{-1} which corresponds to the stretching vibration of hydroxyl groups (νOH) present in water, alcohols, carboxylic acids, and phenols.

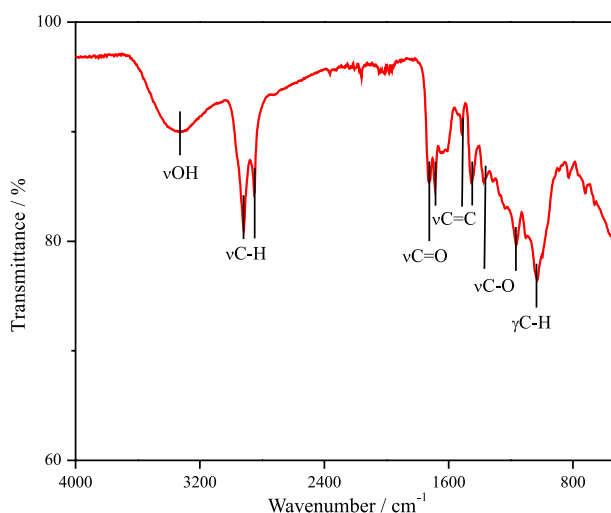


Figure 1. Infrared spectrum (FTIR-ATR) of leaf of *E. grandis*.

The bands at 2918 and 2850 cm^{-1} correspond to asymmetrical and symmetrical stretching ($\nu\text{C-H}$) of $\text{C}_{\text{sp}^3}\text{-H}$ bonds, while the band at 1726 cm^{-1} is related to stretching vibration of carbonyl ($\nu\text{C=O}$) of carboxylic acids. Bands attributed to the C=C bonds present in aromatic compounds were observed at 1685, 1514, and 1456 cm^{-1} . The band at 1034 cm^{-1} was assigned to stretching vibration of alkenes $\text{C}_{\text{sp}^2}\text{-H}$ bonds ($\nu\text{C-H}$), while the bands at 1377 and 1165 cm^{-1} can refer to stretching vibration of ethers ($\nu\text{C-O}$).³³

GC-MS analysis of the methanolic extract from leaves of *E. grandis* allowed the identification of a series of metabolites, which are depicted in Table 1. Four classes of compounds, namely carboxylic acids, phenolic compounds, terpenes, and carbohydrates were detected in

the extract, and all of these chemical classes are described in the literature³⁹ as connected with the synthesis of silver nanoparticles.

For instance, it has been suggested that the tautomeric transformation of flavonoids from the enol form to the ketone form can release H atoms that reduce the metallic

Table 1. Compounds identified in the methanolic extract obtained from the leaves of *E. grandis*

	t_R / min	Compound	Area / %	RI	
				Calculated	Literature
carboxylic acids			0.2		
1	7.22	lactic acid-TMS	–	–	–
2	7.77	glycolic acid-TMS	–	–	–
3	17.25	glyceric acid-TMS	–	1341	1345 ³⁴
4	30.36	<i>cis</i> -aconitic acid-TMS	–	1759	–
5	32.65	tetradecanoic acid-TMS	–	1843	1850 ³⁴
6	37.68	palmitic acid-TMS	0.2	2040	2050 ²⁸
7	41.52	linoleic acid-TMS	–	2202	2212 ²⁸
8	41.77	α -linolenic acid-TMS	–	2213	2210 ³⁵
9	42.23	stearic acid-TMS	–	2233	2248 ³⁵
phenolics			1.1		
10	21.68	eugenol-TMS	–	1472	1464 ³⁶
11	24.82	tyrosol -TMS	–	1571	1579 ³⁷
12	35.14	<i>p</i> -coumaric acid (TMS)	–	1938	1942 ²⁸
13	35.99	gallic acid-TMS	1.1	1971	1881 ³⁴
14	38.98	ferulic acid-TMS	–	2094	2101 ²⁸
terpenes			9.3		
15	10.44	(<i>R</i>)-(+)-citronellal	6.3	1153	1152 ³⁸
16	13.73	L-isopulegol-TMS	0.5	1244	–
17	16.19	citronellol-TMS	1.0	1311	–
18	18.85	citronellic acid-TMS	0.2	1387	–
19	19.75	<i>trans</i> -caryophyllene	0.2	1413	1412 ²⁸
20	22.61	linalool oxide-TMS	0.9	1500	–
21	23.35	linalool oxide-TMS	–	1524	–
22	40.77	phytol-TMS	0.2	2169	2183 ³⁷
23	53.88	squalene	–	2811	2807 ³⁵
carbohydrates			39.7		
24	29.96	xylitol-TMS	0.2	1745	1743 ²⁸
25	31.36	L-fucitol-TMS	0.2	1795	–
26	32.37	D-psicofuranose	3.5	1833	1843 ³⁷
27	32.59	D-fructofuranose	3.1	1841	1848 ²⁸
28	32.65	D-fructose-TMS	1.5	1843	1853 ³⁴
29	34.66	α -D-galactopyranose-TMS	6.7	1919	1900 ³⁷
30	34.69	D-glucopyranose-TMS	2.6	1920	1931 ²⁸
31	35.78	ethyl-D-glucopyranoside-TMS	0.3	1963	–
32	36.51	carbohydrate	1.6	1992	–
33	37.10	D-glucose-TMS	10.7	2015	2031 ²⁸
34	39.57	myo-inositol-TMS	6.2	2118	2127 ³⁴
35	51.66	sucrose-TMS	2.1	2691	2700 ³⁴
other			0.6		
36	15.24	glycerol-TMS	0.6	1285	1290 ²⁸

t_R : retention time; RI: retention index; TMS: trimethylsilyl derivatives.

cation. The conversion of the ketone functional group to carboxylic acid, in some flavonoids, was also previously identified⁴⁰ as a possible candidate for the reduction of Ag^+ . However, upon the comparison of the initial and final compositions of a cucumber extract used in the synthesis of AgNPs, no variation was found in the concentration of phenolic compounds, but variations were observed in the concentration of reducing sugars and organic acids.⁴¹ Such results led to the suggestion that sugars were the main compounds responsible for the synthesis, probably by tautomeric transformations and oxidation of carbohydrate aldehyde groups.^{16,40}

Synthesis and characterization of the AgNPs

The AgNPs were obtained by treatment of silver nitrate aqueous solution with aqueous extract of *E. grandis* leaves at 90 °C. The UV-Vis absorption spectrum obtained for AgNPs is shown in Figure 2, and a picture of both is depicted in the insert. Because of the LSPR phenomenon, it is possible to notice a characteristic band. In general, AgNPs synthesized by plant extracts present a band with maximum absorption wavelength (λ_{max}) between 400-460 nm.³² However, in this work, two convoluted bands were observed, one with λ_{max} at 368 nm and the other at 407 nm, in contrast to previous studies that investigate other eucalypts species for the synthesis of AgNPs: *E. urophylla*, 447 nm; *E. citriodora*, 445 nm; *E. robusta*, 482 nm;²¹ *E. corymbia*, 425 nm;²⁵ *E. globulus*, 428 nm;^{22,24} *E. macrocarpa*, 430 nm;²⁰ *E. chapmaniana*, 413 nm;¹⁹ and *E. camaldulensis*, 420 nm.²³

Organic compounds, especially alkenes, absorb radiation in the ultraviolet region (< 380 nm).⁴² Thus, it

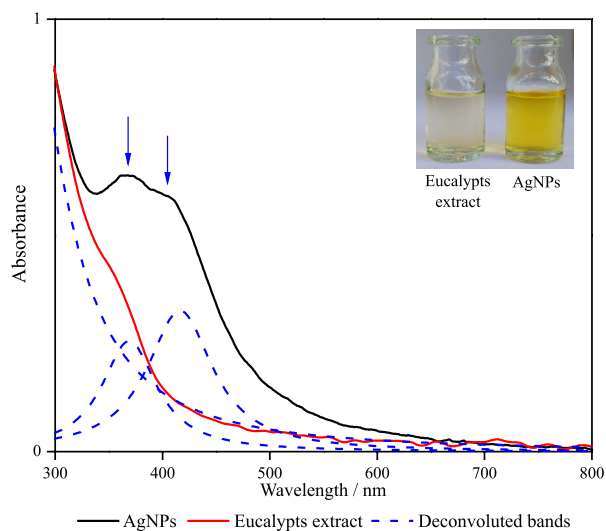


Figure 2. Ultraviolet-visible spectra for AgNPs and aqueous extract of *E. grandis* leaves (eucalypts extract).

is possible that these compounds are responsible for the observed band at this region in the spectrum of the aqueous extract from *E. grandis* contained in Figure 2. However, the characteristic band for AgNPs observed in the spectrum must be emphasized, which indicates their formation.

DLS was used to determine the hydrodynamic diameter of AgNPs in suspension. It is possible to observe in Figure 3, which shows the size distribution of one of the AgNPs, two populations of particles, one with a mean hydrodynamic diameter equal to 1.7 ± 0.1 nm and the other presenting 52.9 ± 14.8 nm. The *E. grandis* extract was also analyzed by DLS revealing a population with an average size equal to 307 ± 47 nm, of unknown nature (Figure 3). Analysis by DLS showed that there was no variation, over a month, in the mean particle size of the two populations of AgNPs previously mentioned (*p*-value ANOVA equal to 0.29 for the particles presenting 1.7 ± 0.1 nm and 0.78 for those with 52.9 ± 14.8 nm).

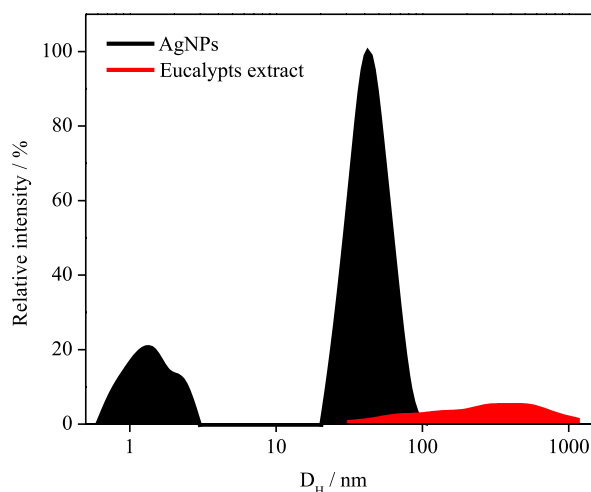


Figure 3. Size distribution graphs (D_H) for AgNPs and aqueous extract of *E. grandis* leaves (eucalypts extract).

Despite being the most suitable technique for evaluating the size of particles in colloidal systems,⁴³ since it generally does not require sample preparations that could introduce artifacts in the analysis, the result provided by the dynamic scattering of light does not necessarily correspond to the actual particle size. This occurs because aggregates are not distinguished from their constituents and the layer adsorbed to the particle can increase its apparent size. Thus, electron microscopy analysis was performed, and the result can be seen in Figure 4.

The mean average of AgNPs diameter was 9.7 ± 0.3 nm, although it was observed that particle sizes ranged from 5 to 50 nm. The particles were spherical and minimal agglomeration was noted indicating that the *E. grandis* extract was well suited for reducing and stabilizing the

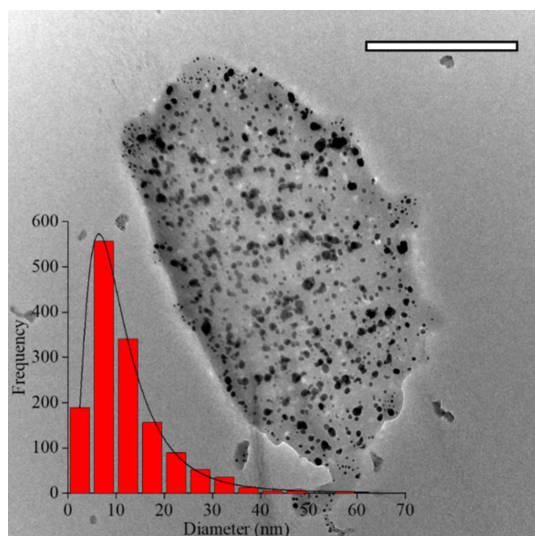


Figure 4. TEM image and frequency distribution histogram of the synthesized AgNPs. Scale bar: 500 nm.

AgNPs. EDS images exhibited the presence of silver alongside carbon, probably due to the organic molecules that are bound to the surface of the AgNPs (Figure 5).

X-ray diffraction can be used to assess the crystallinity of metallic nanoparticles.⁴⁴ In the diffractogram shown in Figure 6, it is possible to observe peaks at 38.25° , 44.20° , 64.70° , and 77.45° which correspond to the respective crystalline planes: (1 1 1), (2 0 0), (2 2 0), and (3 1 1), according to JCPDS 89-3722 standard for the system centered face crystalline of silver. Almost all the works describing the synthesis of AgNPs by plant extracts report this crystal system.³⁹

The results described above indicate that the compounds present in the aqueous extract of *E. grandis* leaves were able to promote the synthesis and stabilization of AgNPs. The nanoparticles were stable for at least one month under ambient conditions. Since one of the main properties of AgNPs is their biological activity, so much so that it is currently the main reason for most commercial applications,⁴⁵ then the antibacterial and leishmanicidal activities of the synthesized AgNPs were evaluated.

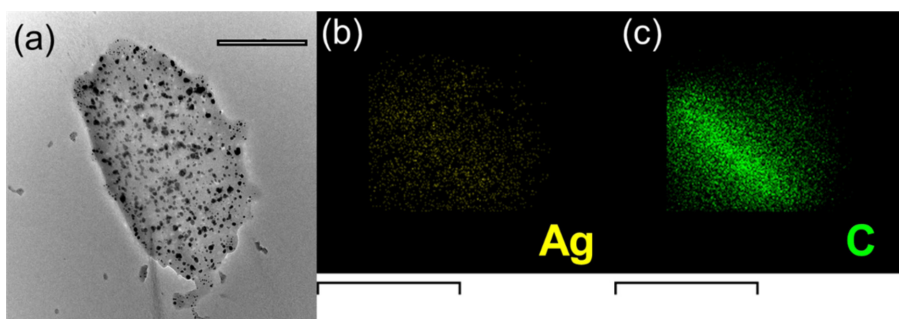


Figure 5. (a) TEM image of the synthesized AgNPs (scale bar: 500 nm) and EDS images of (b) silver and (c) carbon (scale bars: 900 nm) in the same region of (a).

Antibacterial and leishmanicidal activities of AgNPs

The aqueous extract from *E. grandis* leaves presented a reduced activity against *E. coli* but the effect was increased upon exposure of *E. coli* to the suspension of the AgNPs (Figure 7). At a concentration of $53.9 \mu\text{g mL}^{-1}$, the AgNPs inhibited the growth of *E. coli*. A dose-dependent effect was seen on *S. aureus* cells although the activity was significantly lower when compared to *E. coli*. This difference may be caused by features of the cell wall of Gram-positive and Gram-negative bacteria. Thicker cell wall such as those seen in Gram-positives protects antimicrobial agents, in particular metal nanoparticles.⁴⁶ Noteworthy, an aqueous silver nitrate solution with the same silver mass concentration was effective against both bacteria suggesting that the oxidative dissolution of the nanoparticles with the release of Ag^+ ions may be responsible for the biological activity of the AgNPs.^{47,48}

The results reported here differ from previous studies reported by Ali *et al.*²² that used leaves extracts of *E. globulus* for the synthesis of AgNPs. Although a dose-dependent response between the concentration of silver and the antibacterial activity was seen, increased susceptibility of *S. aureus* compared to *E. coli* was observed by the authors. This could be due to the synthesis method used,²² that was assisted by microwaves resulting in particles with smaller sizes and size distribution (according to TEM: 5-25 nm) than those obtained in this study. It has been reported⁴⁹ that AgNPs of smaller size contribute to the antibacterial activity.

Leishmaniasis is a group of more parasitic diseases, which the etiologic agents are over twenty species of protozoan parasites belonging to the genus *Leishmania*. These obligatory intracellular parasites are transmitted to animals and humans through the bites of infected female phlebotomine sandflies. These tropical neglected diseases remain endemic in more than 60 countries and an estimated 0.7-1 million new cases of leishmaniasis *per year* are reported from nearly 100 endemic countries.⁵⁰ Different

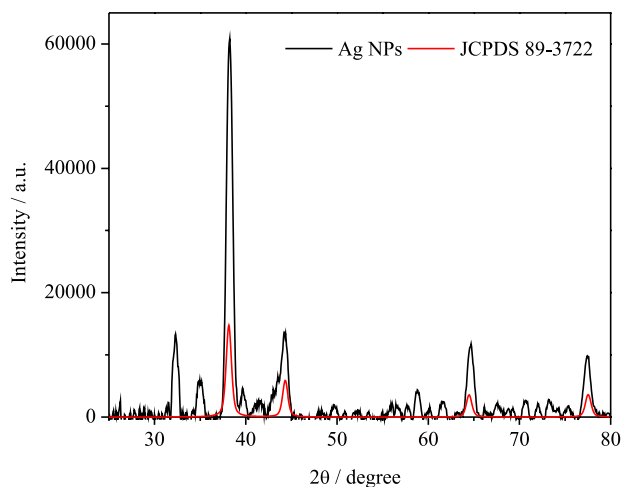


Figure 6. Diffractograms of AgNPs and Ag pattern JCPDS 89-3722.

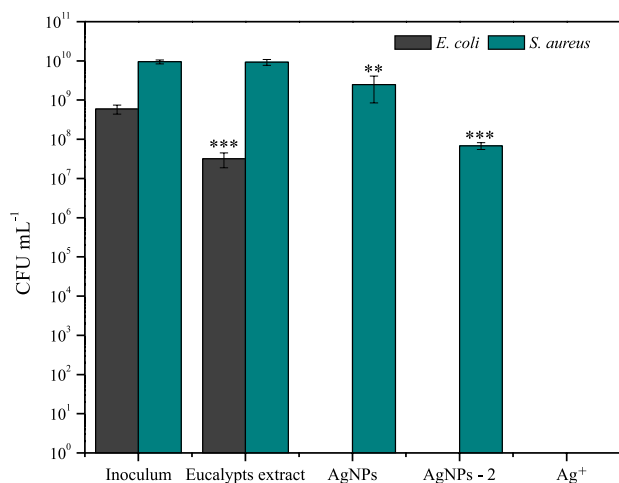


Figure 7. Antibacterial activity of AgNPs synthesized in this work. Bacteria were grown in the presence of aqueous extract of *E. grandis* (eucalypts extract), AgNPs ($26.9 \mu\text{g mL}^{-1}$), AgNPs-2 ($53.9 \mu\text{g mL}^{-1}$) and a solution of silver nitrate (Ag^+ , $26.9 \mu\text{g mL}^{-1}$). Inoculum refers to the bacterial growth in Mueller-Hinton media (** $p \leq 0.01$, *** $p \leq 0.001$).

clinical manifestations of leishmaniasis are known, namely visceral, cutaneous, and mucocutaneous. They depend on the parasite species and the host parasite relationship.⁵¹ There are several drugs that have been used in the treatment of leishmaniasis, such as sodium stibogluconate, meglumine antimoniate, miltefosine, amphotericin B, and pentamidine. However, these drugs present several problems associated with them such as severe side effects, high toxicity, and high cost.^{52,53} Therefore, the development of new, safer, and cheaper drug treatments for leishmaniasis is urgently needed.

Herein, the AgNPs were evaluated against promastigote form of *Leishmania infantum* (MHOM/BR/1970/BH46) which causes visceral leishmaniasis as well as against *Leishmania braziliensis* (MHOM/BR/75/M2904) and *Leishmania amazonensis* (IFLA/BR/1967/PH-8) which

cause cutaneous leishmaniasis. The results are presented in Table 2.

Table 2. Effect of AgNPs on promastigote forms of *L. infantum*, *L. braziliensis* and *L. amazonensis*. Amphotericin B was used as positive control

	Promastigote growth inhibition / %		
	<i>L. infantum</i>	<i>L. braziliensis</i>	<i>L. amazonensis</i>
Volume of AgNP suspension / μL			
0	0	0	0
10	17.4	0	0
50	35.3	0	0
80	57.6	4.30	2.34
100	59.9	26.2	6.34
150	67.9	40.1	28.1
Volume of amphotericin B / μL			
1	66.7	59.1	25.2
2	70.6	68.0	30.4
4	75.3	69.1	55.6
R ²	0.9009	0.9284	0.9051

R²: coefficient of determination.

As can be noticed, the effect of the AgNPs on the promastigote forms is dependent on the volume of suspension; as it increases, the percentage of growth inhibition also enhances. *L. infantum*, which causes visceral leishmaniasis, was more sensitive to the treatments with AgNPs as compared to *L. amazonensis* and *L. braziliensis*. If not treated, visceral leishmaniasis can result in the death of the infected human or animal. Even though the AgNPs were less effective than amphotericin B, it deserves comment the fact that for some treatments the nanoparticles were equipotent to amphotericin B. For instance, when treated with 150 μL of AgNPs suspension, the inhibition percentage of *L. infantum* was similar to the treatment with 1 or 2 μL of amphotericin B.

Conclusions

In summary, it can be concluded that AgNPs were obtained from a process that employed the aqueous extract of *E. grandis* leaves. The nanoparticles showed antibacterial activity against *E. coli* as well as on *Leishmania infantum*, *Leishmania braziliensis*, and *Leishmania amazonensis*. *L. infantum* was more sensitive to the nanoparticles. *E. grandis* leaves can be used to obtain a product with added value, which, in general, gives a more noble application to a vegetable residue. Such residue, when used, is intended only for obtaining essential oil. In addition, the process used in

this work is aligned with some principles of green chemistry, for example, the use of water as a solvent and renewable raw material and has the potential to be economically viable.

Acknowledgments

The authors thank the Coordenação de Aperfeiçoamento de Pessoal de Nível Superior - Brazil (CAPES), Conselho Nacional de Desenvolvimento Científico e Tecnológico (CNPq), Fundação de Amparo à Pesquisa do Estado de Minas Gerais (FAPEMIG), CNPq/FAPEMIG (agreement registered in SICONV: 793988 / 2013), Department of Chemistry of Universidade Federal de Viçosa, Physics Department of Universidade Federal de Viçosa, and the Center of Microscopy at the Universidade Federal de São Carlos for providing the equipment and technical support for experiments involving electron microscopy; and Professor Eduardo Borges from the Departamento de Engenharia Florestal of Universidade Federal de Viçosa for the taxonomic identification and provision of the *E. grandis* leaves.

Author Contributions

Lucas M. F. Oliveira was responsible for the conceptualization, data curation, formal analysis, investigation, validation, visualization, writing original draft; Ueveton P. da Silva for the formal analysis, investigation, validation; João Pedro V. Braga for the formal analysis, investigation, validation; Álvaro V. N. C. Teixeira for the formal analysis funding acquisition, investigation, project administration, writing-review and editing; Andréa O. B. Ribon for the formal analysis funding acquisition, investigation, project administration, writing-review and editing; Eduardo V. V. Varejão for the formal analysis, funding acquisition, investigation, project administration, writing-review and editing; Eduardo A. F. Coelho for the formal analysis, investigation, validation; Camila S. de Freitas for the formal analysis, investigation, validation; Róbson R. Teixeira for the formal analysis funding acquisition, investigation, project administration, writing-review and editing; Renata P. L. Moreira for the formal analysis funding acquisition, investigation, project administration, writing-review and editing.

References

- Gahlawat, G.; Choudhury, A. R.; *RSC Adv.* **2019**, *9*, 12944. [Crossref]
- Jain, S.; Mehata, M. S.; *Sci. Rep.* **2017**, *7*, 15867. [Crossref]
- Dong, X.-Y.; Gao, Z.-W.; Yang, K.-F.; Zhang, W.-Q.; Xu, L.-W.; *Catal. Sci. Technol.* **2015**, *5*, 2554. [Crossref]
- Xu, G.; Lin, G.; Lin, S.; Wu, N.; Deng, Y.; Feng, G.; Chen, Q.; Qu, J.; Chen, D.; Chen, S.; Niu, H.; Mei, S.; Yong, K. T.; Wang, X.; *Sci. Rep.* **2016**, *6*, 37677. [Crossref]
- Alshehri, A. H.; Jakubowska, M.; Młodziński, A.; Horaczek, M.; Rudka, D.; Free, C.; Carey, J. D.; *ACS Appl. Mater. Interfaces* **2012**, *4*, 7007. [Crossref]
- Gu, M.; Zhang, Q.; Lamon, S.; *Nat. Rev. Mater.* **2016**, *1*, 16070. [Crossref]
- Chow, E. K.-H.; Ho, D.; *Sci. Transl. Med.* **2013**, *5*, 216rv4. [Crossref]
- Arvizo, R. R.; Bhattacharyya, S.; Kudgus, R. A.; Giri, K.; Bhattacharya, R.; Mukherjee, P.; *Chem. Soc. Rev.* **2012**, *41*, 2943. [Crossref]
- Xiong, Y.; Lu, X.; *Metallic Nanostructures: from Controlled Synthesis to Applications*; Springer International Publishing: Cham, 2015.
- Rycenga, M.; Cobley, C. M.; Zeng, J.; Li, W.; Moran, C. H.; Zhang, Q.; Qin, D.; Xia, Y.; *Chem. Rev.* **2011**, *111*, 3669. [Crossref]
- El-Nour, K. M. M. A.; Eftaiha, A.; Al-Warthan, A.; Ammar, R. A. A.; *Arabian J. Chem.* **2010**, *3*, 135. [Crossref]
- Awad, M. A.; Al Olayan, E. M.; Siddiqui, M. I.; Merghani, N. M.; Alsaiif, S. S. A.; Aloufi, A. S.; *Biomed. Pharmacother.* **2021**, *137*, 111294. [Crossref]
- Allahverdiyev, A. M.; Abamor, E. S.; Bagirova, M.; Ustundag, C. B.; Kaya, C.; Kaya, F.; Rafailovich, M.; *Int. J. Nanomed.* **2011**, *6*, 2705. [Crossref]
- Ahmed, S.; Ahmad, M.; Swami, B. L.; Ikram, S.; *J. Adv. Res.* **2016**, *7*, 17. [Crossref]
- Hebbalalu, D.; Lalley, J.; Nadagouda, M. N.; Varma, R. S.; *ACS Sustainable Chem. Eng.* **2013**, *1*, 703. [Crossref]
- Akhtar, M. S.; Panwar, J.; Yun, Y. S.; *ACS Sustainable Chem. Eng.* **2013**, *1*, 591. [Crossref]
- Salehi, B.; Sharifi-Rad, J.; Quispe, C.; Llaique, H.; Villalobos, M.; Smeriglio, A.; Trombetta, D.; Ezzat, S. M.; Salem, M. A.; Zayed, A.; Castillo, C. M. S.; Yazdi, S. E.; Sen, S.; Acharya, K.; Sharopov, F.; Martins, N.; *Trends Food Sci. Technol.* **2019**, *91*, 609. [Crossref]
- Barbosa, L. C. A.; Filomeno, C. A.; Teixeira, R. R.; *Molecules* **2016**, *21*, 1671. [Crossref]
- Sulaiman, G. M.; Mohammed, W. H.; Marzoog, T. R.; Al-Amiery, A. A. A.; Kadhum, A. A. H.; Mohamad, A. B.; *Asian Pac. J. Trop. Biomed.* **2013**, *3*, 58. [Crossref]
- Poinern, G. E. J.; Chapman, P.; Shah, M.; Fawcett, D.; *Nano Bull.* **2013**, *2*, 130101.
- Mo, Y.; Tang, Y.; Wang, S.; Lin, J.; Zhang, H.; Luo, D.; *Mater. Lett.* **2015**, *144*, 165. [Crossref]
- Ali, K.; Ahmed, B.; Dwivedi, S.; Saquib, Q.; Al-Khedhairi, A. A.; Musarrat, J.; *PLoS One* **2015**, *10*, e0131178. [Crossref]
- Mohammed, A. E.; *Asian Pac. J. Trop. Biomed.* **2015**, *5*, 382. [Crossref]
- Balamurugan, M.; Saravanan, S.; *J. Inst. Eng.: Ser. A* **2017**, *98*, 461. [Crossref]
- Sila, M. J.; Nyambura, M. I.; Abong'o, D. A.; Mwaura, F. B.; Iwuoha, E.; *Nano Hybrids Compos.* **2019**, *25*, 32. [Crossref]

26. da Silva, U. P.; Furlani, G. M.; Demuner, A. J.; da Silva, O. L. M.; Varejão, E. V. V.; *Nat. Prod. Res.* **2019**, *33*, 2681. [Crossref]
27. Isidorov, V. A.; Rusak, M.; Szczepaniak, L.; Witkowski, S.; *J. Chromatogr. A* **2007**, *1166*, 207. [Crossref]
28. Isidorov, V. A.; Lech, P.; Żółciak, A.; Rusak, M.; Szczepaniak, L.; *Trees* **2008**, *22*, 531. [Crossref]
29. *Dynamic Light Scattering Software*, v.5.89; Brookhaven Instruments, USA, 2012.
30. *Crystallographica Search-Match*, v.2.1.1.1; Oxford Cryosystems, UK, 2004. [Link] accessed in September 2022
31. Coelho, E. A. F.; Tavares, C. A. P.; Carvalho, F. A. A.; Chaves, K. F.; Teixeira, K. N.; Rodrigues, R. C.; Charest, H.; Matlashewski, G.; Gazzinelli, R. T.; Fernandes, A. P.; *Infect. Immun.* **2003**, *71*, 3988. [Crossref]
32. Mikhailov, O. V.; Mikhailova, E. O.; *Materials* **2019**, *12*, 3177. [Crossref]
33. Coates, J. In *Encyclopedia of Analytical Chemistry*; Meyers, R. A.; McKelvy, M. L., eds.; John Wiley & Sons, Ltd: Chichester, UK, 2006. [Crossref]
34. Isidorov, V. A.; Kotowska, U.; Vinogorova, V. T.; *Anal. Sci.* **2005**, *21*, 1483. [Crossref]
35. Silva, J. G. A.; Silva, A. A.; Coutinho, I. D.; Pessoa, C. O.; Cavalheiro, A. J.; Silva, M. G. V.; *J. Braz. Chem. Soc.* **2016**, *27*, 1872. [Crossref]
36. Jen, C. N.; Hatch, L. E.; Selimovic, V.; Yokelson, R. J.; Weber, R.; Fernandez, A. E.; Kreisberg, N. M.; Barsanti, K. C.; Goldstein, A. H.; *Atmos. Chem. Phys.* **2019**, *19*, 1013. [Crossref]
37. Isidorov, V. A.; *GC-MS of Biologically and Environmentally Significant Organic Compounds: TMS Derivatives*, 1st ed.; John Wiley & Sons Ltd.: New Jersey, 2020.
38. Shellie, R.; Marriott, P.; Zappia, G.; Mondello, L.; Dugo, G.; *J. Essent. Oil Res.* **2003**, *15*, 305. [Crossref]
39. Tarannum, N.; Divya; Gautam, Y. K.; *RSC Adv.* **2019**, *9*, 34926. [Crossref]
40. Makarov, V. V.; Love, A. J.; Sinitsyna, O. V.; Makarova, S. S.; Yaminsky, I. V.; Taliansky, M. E.; Kalinina, N. O.; *Acta Nat.* **2014**, *6*, 35. [Link] accessed in September 2022
41. Zhang, H.; Huang, Y.; Gu, J.; Keller, A.; Qin, Y.; Bian, Y.; Tang, K.; Qu, X.; Ji, R.; Zhao, L.; *New J. Chem.* **2019**, *43*, 3946. [Crossref]
42. Passos, M. L. C.; Sarraguça, M. C.; Saraiva, M. L. M. F. S.; Rao, T. P.; Biju, V. M. In *Encyclopedia of Analytical Science*, 3rd ed.; Worsfold, P.; Poole, C.; Townshend, A.; Miró, M., eds.; Academic Press: Oxford, UK, 2019, p. 350-359.
43. Ribeiro, L. N. M.; Couto, V. M.; Fraceto, L. F.; de Paula, E.; *Sci. Rep.* **2018**, *8*, 982. [Crossref]
44. Vijayaraghavan, K.; Ashokkumar, T.; *J. Environ. Chem. Eng.* **2017**, *5*, 4866. [Crossref]
45. Syafiuddin, A.; Salmiati; Salim, M. R.; Kueh, A. B. H.; Hadibarata, T.; Nur, H.; *J. Chin. Chem. Soc.* **2017**, *64*, 732. [Crossref]
46. Slavin, Y. N.; Asnis, J.; Häfeli, U. O.; Bach, H.; *J. Nanobiotechnol.* **2017**, *15*, 65. [Crossref]
47. Le Ouay, B.; Stellacci, F.; *Nano Today* **2015**, *10*, 339. [Crossref]
48. Roy, A.; Bulut, O.; Some, S.; Mandal, A. K.; Yilmaz, M. D.; *RSC Adv.* **2019**, *9*, 2673. [Crossref]
49. Liao, C.; Li, Y.; Tjong, S.; *Int. J. Mol. Sci.* **2019**, *20*, 449. [Crossref]
50. Burza, S.; Croft, S. L.; Boelaert, M.; *Lancet* **2018**, *392*, 951. [Crossref]
51. David, C. V.; Craft, N.; *Dermatol. Ther.* **2009**, *22*, 491. [Crossref]
52. Iqbal, H.; Ishfaq, M.; Wahab, A.; Abbas, M. N.; Ahmad, I.; Rehman, A.; Zakir, M.; *Asian Pac. J. Trop. Dis.* **2016**, *6*, 1. [Crossref]
53. Santos, D. O.; Coutinho, C. E. R.; Madeira, M. F.; Bottino, C. G.; Vieira, R. T.; Nascimento, S. B.; Bernardino, A.; Bourguignon, S. C.; Corte-Real, S.; Pinho, R. T.; Rodrigues, C. R.; Castro, H. C.; *Parasitol. Res.* **2008**, *103*, 1. [Crossref]

Submitted: April 15, 2022

Published online: October 6, 2022

